Doping of Polyaniline by Transition-Metal Salts

O. P. Dimitriev†

Institute of Semiconductor Physics, National Academy of Sciences of Ukraine, pr. Nauki 45, Kiev 03028, Ukraine

Received November 7, 2003; Revised Manuscript Received January 31, 2004

ABSTRACT: Complexes of some transition-metal salts and emeraldine base of polyaniline were synthesized and characterized by UV−vis−IR spectroscopy, morphology studies, and conductivity measurements. Depending on the inorganic salt used, two extreme cases of doping were distinguished. The first regime of doping resulted in films of grained morphology, with a relatively high conductivity of up to 10^{-1} S/cm and electronic absorption spectra showing features of both pseudo-protonic doping and oxidation of the polymer backbone. IR absorption spectra were consistent with interaction of the benzenoid groups of the polymer with metal cations. The second regime of doping resulted in a smoother film morphology without grains, but with poor conductivity, normally not more than 10^{-3} S/cm, and higher solvent concentration in the film. Electronic and IR absorption spectra were consistent with pseudo-protonation of the polymer backbone. On the basis of the obtained data, a model of the macromolecular polyaniline−transition-metal salt complex is proposed.

1. Introduction

Polyaniline (PANI) has attracted considerable attention due to its unique properties, in particular its reversibly controlled conversions via redox doping and protonation. An insulating emeraldine base (EB) form of PANI can be converted to the conducting form by exposure to protonic acids resulting in an increase of conductivity by more than 10 orders of magnitude. The result of protonation is schematically shown in Figure 1.

Although the protonation is the simplest way for getting a highly conductive PANI, it is not the only way. There are a few other methods which allow to convert the EB form of PANI to its conductive form. One of them is the employment of Lewis acids as dopants, for example $SnCl_4$[1] or BF_3,[2] which yield an increase of conductivity of PANI films up to about 20 S/cm at room temperatures.[2]

The other way to achieve highly conductive PANI films is to employ alkali-metal salts as dopants.[3,4] Light metal ions, such as Li^+ or Na^+, are able to coordinate to imine nitrogen atoms of the polymer backbone, thus playing the role of protons and leading to a pseudo-protonation of the polymer. However, because of the mass difference of the metal ion and the proton, the highly symmetrical structure of the polymer backbone is not possible upon doping with alkali-metal ions, and as a result, the conductivity of PANI films doped by alkali-metal salts is lower by several orders of magnitude as compared with that of the protonic acid doped films.

Finally, the EB form of PANI can be converted to the conductive form via oxidative doping at the amine nitrogen atoms. Examples of such dopants are $FeCl_3$[5] and $EuCl_3$.[6] In the latter case, the conductivity of doped PANI films approaches that of the hydrochloric acid doped films, and this phenomenon was explained via successive oxidation, pseudo-protonation, and protonation of the polymer backbone during doping.[6]

In addition to the above salts, which serve as dopants, there are salts of other metals which have electrode potentials intermediate between that of alkali-metal ions and that of oxidative metal ions. It appears that such ions cannot directly oxidize EB chains or to function as protons. Therefore, their influence on the polymer chain needs to be studied more carefully. There were several papers reporting the effect of doping of EB by various transition-metal salts,[5,7−12] where the mechanism of doping by these salts was assigned to either pseudo-protonation or Lewis acid doping of the polymer backbone.

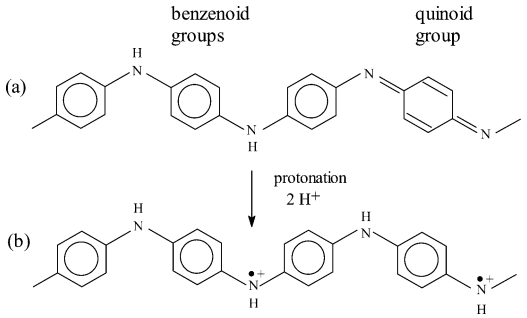

Figure 1. Scheme of protonation of the EB form of PANI. Acid counterions are not shown.

On the other hand, understanding of the mechanisms of interaction of PANI and metal ions leads to the potential application of the polymer/metal pair in various fields such as organic electronics, where PANI/metal heterojunctions are employed for electrical transport and rectification,[13] as protective coatings against corrosion of metal surfaces,[14−16] as redox-active catalysts for inducing chemical reactions in coordination chemistry,[17,18] in separation and recovery of noble metals,[19] etc. PANI can be used as a model polymer for the study of the above interactions, because its backbone consists of two basic groups possessing different activity in respect to metal cations, namely the electron-rich benzenoid group and the electron-deficient quinoid group, respectively (Figure 1).

This paper aims to clarify the effect of doping of PANI films by transition-metal salts in more detail. Recently, we reported that EB can interact with many transition-metal salts, resulting in formation of an insoluble

† E-mail: dimitr@isp.kiev.ua.

10.1021/ma035677w CCC: $27.50
Published on Web 04/08/2004

precipitate in DMFA solutions.[20] In this work, we prepare EB:metal salt complexes in the form of films in order to determine their conductivities directly.

2. Experimental Section

2.1. Sample Preparation. Emeraldine base (EB) of polyaniline was dissolved in *N*-methylpyrrolidinone (NMP) to prepare a stock solution with concentration of 1 wt %, followed by treatment of the solution in the ultrasonic bath and filtering of the solution to remove undissolved particles. Salts of $FeSO_4$, $FeCl_3$, $MnCl_2$, $NiCl_2$, $CuCl_2$, $ZnCl_2$, $CdCl_2$, $LaCl_3$, $EuCl_3$, $La(NO_3)_3$, $Eu(NO_3)_3$, $Sm(NO_3)_3$, and $Nd(NO_3)_3$ were dissolved in NMP to prepare solutions with desirable concentrations.

EB−metal salt complex solutions were prepared by mixing the EB and salt solutions with certain proportion of EB (calculated per tetramer units) to metal ions. The mixture usually consisted of 40 mL of the EB stock solution and 10 mL of the salt solution with concentration of 10^{-1} M that provided an approximate ratio 1:2 of a tetramer unit of the EB to metal cations. Other polymer-to-salt ratios and polymer concentrations were also probed to prepare samples. The solutions were used for the preparation of films by drop-casting onto quartz plates, followed by measurement of electronic absorption spectra and conductivity of these films. For IR measurements, the films were cast onto germanium plates.

2.2. Measurements. Electronic absorption spectra were measured in the transmission and diffusion reflection mode. For the transmission mode, a light beam was set perpendicular to the sample surface, and a bare substrate served as a reference. The diffusion reflection spectra were measured using a collecting sphere. Pellets of the MgO powder served as a reference. The diffusion reflection spectra were taken from the surface of rough samples only to evaluate a scattered signal that can distort the absorption spectra in the transmission mode.

IR absorption spectra were measured in the transmission mode, a bare germanium plate served as a reference. Spectrophotometers SPECORD M40 and SPECORD M80 were used for the measurements in the UV−vis and IR ranges, respectively. Measurements were performed in the ranges of characteristic absorption of the polymer, i.e., in the 330−800 nm region and in the 1700−700 cm^{-1} region, respectively.

The electrical in-plane conductivity of the films was measured using a standard four-probe technique. During the measurement, an appropriate constant current, J, in the range 0.1−10 μA was maintained on two outer probes, and the voltage drop, V, was measured across two inner probes, using a UNI-T M890C$^+$ electrometer. The resulting conductivity, σ, was found according to the formula

$$\sigma = \ln 2\ (J/\pi\ d\ V) \qquad (1)$$

where d is the film thickness.

Film thickness was evaluated through measurements of interference spectra of the samples in the IR range. In this experiment, three equal films of the material with the diameters of 5 mm were deposited at the periphery of a germanium disk of the diameter of 25 mm. This assembly was covered with the other bare disk, so that the films served as a spacer to form an empty gap in the central area between the disks. The interference pattern of the gap was then recorded in the geometry when the IR beam was set perpendicularly to the surface of the disks. The film thickness was equal to that of the gap and was calculated according to the formula[21]

$$d = 5000m/(\nu_1 - \nu_2) \qquad (2)$$

where m is the number of interference maxima between signals ν_1 and ν_2, with ν_1 and ν_2 being the positions of the two interference maxima on the wavenumber scale (in cm^{-1}). In this case, d is expressed in micrometers. The final film thickness on quartz plates was calculated with account of different diameters of the films prepared on the quartz and germanium surfaces.

Film surface morphology was studied by atomic force microscope (AFM), a NanoScope IIIa Dimension 3000 model was used for these studies. The AFM measurements were performed in air and at room temperature. The images were measured in contact mode by working in constant force mode.

3. Results

3.1 Formation of Complex Films. A doped PANI film is obtained by mixing PANI and inorganic salt solutions in NMP and then drop-casting the mixed solution into film at ambient conditions. A slow solvent evaporation, from a few hours to a few days, allowed us to monitor a gradual formation of the film morphology. On formation of films, the dark-blue color of the inorganic salt−polymer mixture changed. This change indicates that interaction of the polymer and inorganic salt occurs in the condensed state, when metal cations change their coordination from solvent to the polymer molecules upon solvent removal. In addition, conductivity of the films increases dramatically as compared with films of pure PANI. The doping is not caused by the protonic acid, which might have formed accidentally as a result of salt hydrolysis in the presence of water traces in the solvent or in the film. As was established earlier,[6] dopant, i.e., the salt, can be removed from the sample by rinsing it with water, with the recovery of the blue color of the undoped EB film, whereas no such dedoping can be obtained in the acid-doped samples.

We roughly distinguish two opposite regimes of doping or two different groups of the transition-metal salts that yield different film morphologies. The first group of salts resulted in homogeneous doping, i.e., the changed color of the doped film was uniform over film surface and, depending on the dopant, was gray, blue-gray, or greenish. This kind of doping yielded a grained film structure, with grains of several tens of nanometers in size, which are densely scattered over the film area, forming larger domains (Figure 2, parts a and c). Numerous defects in the form of holes and cracks were also seen in such a structure.

The second group of salts resulted in heterogeneous doping, when the film color changed over the film area, from blue at the periphery to green in the central area, pointing to a poor miscibility of the polymer and dopant solutions. Morphology of these films were found to be also heterogeneous; however, no grains were found in the film structure (Figure 2b).

Prominent representatives of dopants resulting in the above two regimes of doping were found to be $NiCl_2$, $LaCl_3$, and $EuCl_3$, on one hand, and $ZnCl_2$, $CdCl_2$, and $FeSO_4$, on the other hand. It was found that other salts used in this study, for example, nitrates of rare-earth metals, yield intermediate cases of doping and cannot be unambiguously related to the above groups.

A particularly interesting property of the film formation was the kinetics of solvent evaporation during film casting. It was found that films obtained as a result of the second regime of doping had comparable or larger times of formation, i.e., that time when film surface did not change anymore, as compared with films of pure EB, under the same preparation conditions and solution volumes used. IR spectra of such films showed a considerable amount of solvent residue in the film. On the other hand, films prepared as a result of the first regime of doping showed surprisingly faster kinetics of solvent evaporation (Table 1), with far less solvent residue in the final film, as was determined through their IR spectra. The different regimes of doping cor-

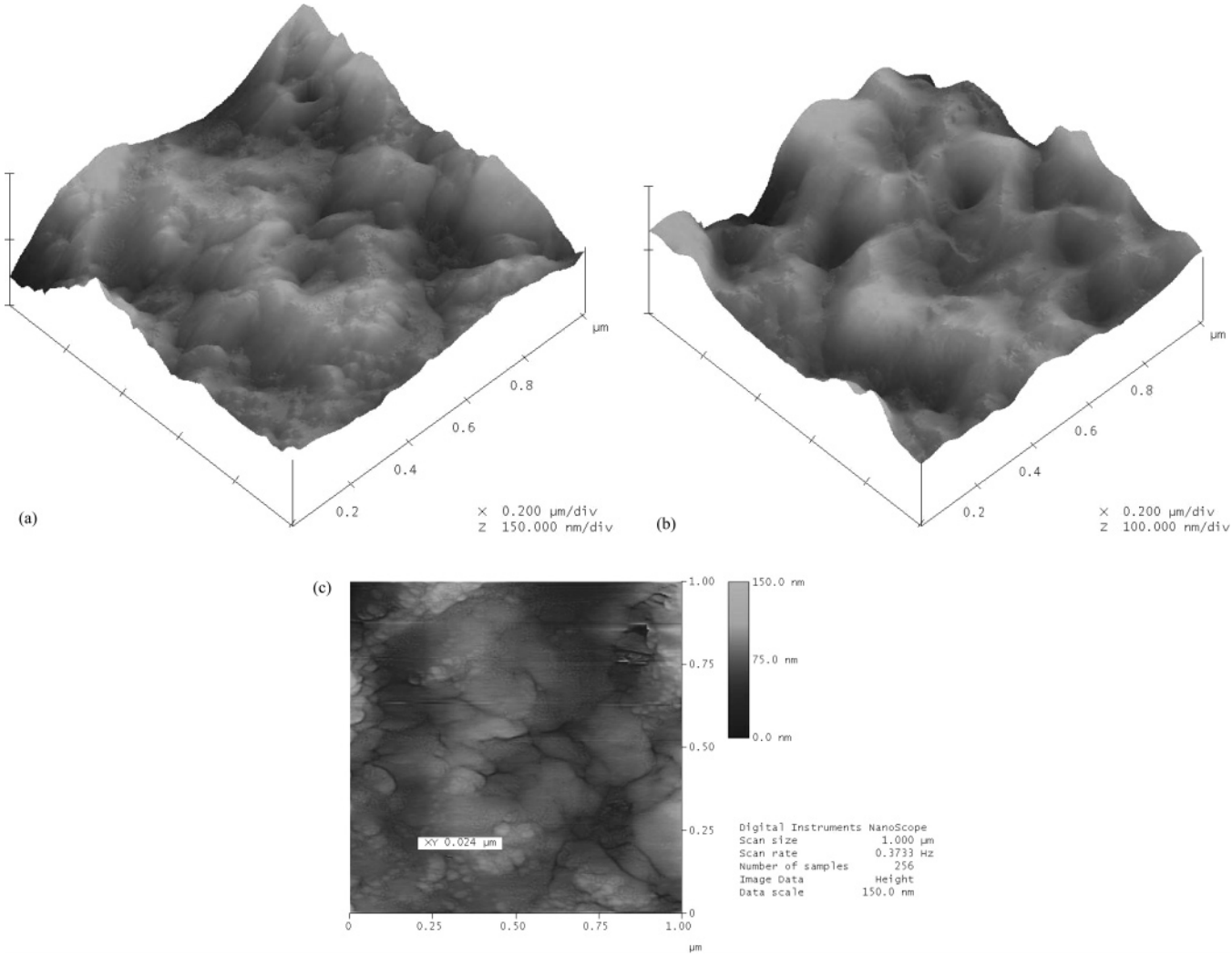

Figure 2. AFM images of (a) $NiCl_2$-doped and (b) $ZnCl_2$-doped PANI film; (c) contrast enhancement of Figure 2a.

Table 1. Comparison of the Film Formation Times as a Result of Spontaneous Evaporation of NMP from Equal Amounts (10 μM) of Complex Solutions Deposited on Glass Substrate at Room Temperature (22 °C) and 45% Environmental Humidity

Film Material (Evaporation Time, h)			
EB:$EuCl_3$	EB:$NiCl_2$	EB:$LaCl_3$	EB
(18.5 ± 0.5)	(19 ± 0.5)	(22.5 ± 0.5)	(22 ± 0.5)
EB:$Eu(NO_3)_3$	EB:$ZnCl_2$	EB:$La(NO_3)_3$	EB:$CdCl_2$
(22 ± 1)	(21 ± 1)	(27 ± 1)	(25.5 ± 0.5)

related well with different tendencies of the solutions to form precipitates. EB solutions with salts of $EuCl_3$, $NiCl_2$, and $LaCl_3$ formed precipitates when left from several days to several weeks in the closed vessel. In some cases, we observed separation of the polymer from the solvent in a few minutes when a solution drop was deposited onto a solid substrate. It seems that the tendency for the polymer complex to be separated from a solvent is responsible for the formation of the grained morphology of the film, with a smaller amount of solvent residue in the film. On the other hand, a great amount of solvent entrapped in films obtained by the second regime of doping plasticizes the film and yields a smoother morphology, i.e., without grains and cracks.

3.2. Effect of Counterions. Although metal cations were found to affect the doping dramatically, a change of the counterion was found to also affect the regime of doping. It was found that nitrate anions adsorb more solvent in the film and retard NMP evaporation during film formation than chloride anions. Nitrate anions were found to also suppress the formation of precipitates in the complex EB solutions. For example, the solution of EB:$Eu(NO_3)_3$ was found to be homogeneous during several months in contrast to solutions of EB:$EuCl_3$, where a dark precipitate formed in a few weeks. IR spectra of films with nitrate salts confirmed a greater amount of NMP residue in the films. The conductivity of films doped by nitrates was found to be usually 1 or 2 orders of magnitude smaller as compared with films doped by the chlorides. Thus, a specific effect of counterions was assigned to their different ability to bind with solvent molecules and thus to affect film morphology and conductivity.

3.3. Conductivity. Electrical conductivity of the complex films was found to be in the range of 10^{-1}–10^{-4} S/cm. The conductivity of films doped by the same salt can vary within 1−2 orders of magnitude, depending on the preparation conditions of the films, i.e., on concentration of the initial polymer solution, relationship of the polymer and salt, aging of the solution, rate of solvent evaporation during film casting, and film thickness, as well as storage time of the samples.

The current passing through the grained samples was found to be unstable, showing leaps up to 10% around an average value, while the current through samples prepared by the second regime of doping was more

Table 2. Conductivity of the Complex Films

Film Material (Conductivity, S cm^{-1})				
EB:HCl	EB:$EuCl_3$	EB:$NiCl_2$	EB:$LaCl_3$	EB:$FeCl_3$
(1×10^0)	(1×10^{-1})	(4×10^{-2})	(2×10^{-2})	(3×10^{-1})
EB:$CdCl_2$	EB:$Eu(NO_3)_3$	EB:$ZnCl_2$	EB:$Sm(NO_3)_3$	EB:$CuCl_2$
(2×10^{-3})	(4×10^{-3})	(1×10^{-3})	(2×10^{-4})	(3×10^{-4})

stable. The instability seems to be due to changes of current pathways in the grained structure. More detailed electrical characteristics of the films are given in a separate paper.[22]

The most surprising feature of the conductivity was its significant change with time. Conductivity of the as-prepared samples usually increased with time by 1−2 orders of magnitude during several weeks or several months depending on the film composition, followed by its decrease probably due to conventional degradation of the polymer material.[23] The conductivity increase for samples doped by the second group of dopants or nitrates was considerably slower as compared with films doped by the first group of dopants. This phenomenon was assigned to a slow release of solvent molecules from the films leading to better interaction of the dopant and polymer molecules. As was mentioned, the amount of solvent residue is dependent on the film composition, so the solvent release occurs with the different rates. The temporal change of the conductivity did not allow to define the film conductivity exactly. Table 2 indicates typical values of conductivity obtained in our experiments for selected samples.

Several facts indicate that conductivity in the complex films is not of the ionic type. The contribution of the ionic transport results in gradual decrease of conductivity during measurements toward a saturation value, and also the ionic transport should increase in the moistened samples. None of these features of the ionic conductivity was found. As was mentioned, conductivity increased with time as the sample lost solvent molecules as compared with the as-prepared, virtually moistened sample. When some samples were exposed to water vapor during measurements, no noticeable changes in conductivity was found. This shows that environmental humidity is not responsible for a slow increase of conductivity with time.

3.4. Electronic Spectra. Electronic absorption spectra of the doped samples can be divided into two groups, in conformity with the two regimes of doping. The first group of spectra, i.e., the spectra from as-prepared films doped by the first group of salts, contained features of both the emeraldine salt (ES) and pernigraniline base (PB) forms of PANI. The ES form of the polymer possesses a polaron absorption near 440 nm and an absorption tail in the near-IR; those features are clearly seen in spectra of films doped by $EuCl_3$ and $NiCl_2$ salts (Figure 3). In addition, these spectra show the presence of a benzenoid-to-quinoid electronic transition (BQET) of the polymer which is blue-shifted to ∼550 nm. Such a shift indicates a partial oxidation of the polymer backbone, i.e., the EB-to-PB conversion.[24,25] Samples doped by copper salts showed typical features of the oxidized form of the polymer, with only a slight polaron absorption band visible as a shoulder at ∼770 nm (Figure 4). Samples prepared by the second regime of doping showed electronic absorption properties similar to the features of acid-protonated PANI films,[26−28] i.e., a strong polaron absorption at ∼440 nm and an absorption tail extending to the IR region, with a complete suppression of the BQET band at ∼600 nm (Figure 4, curve 2).

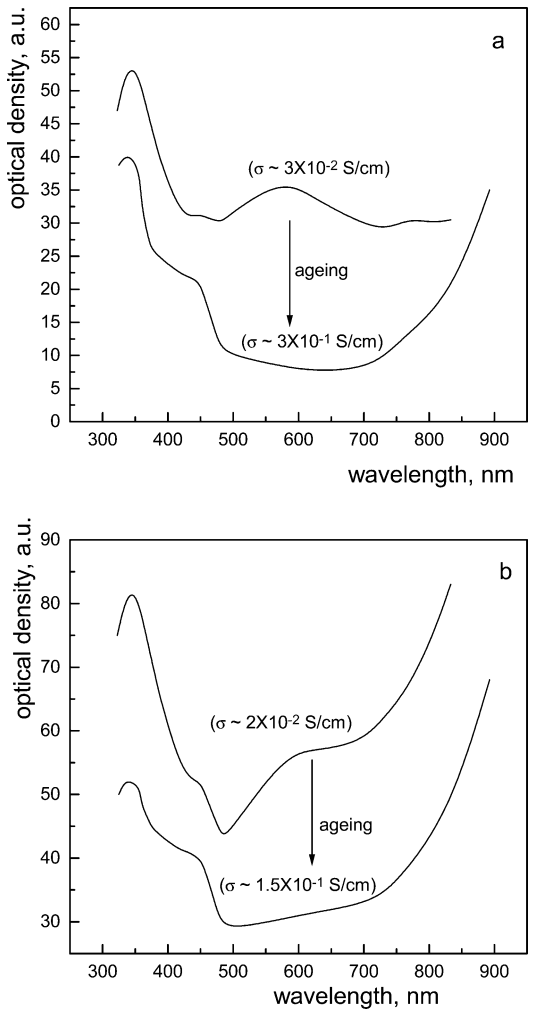

Figure 3. Electronic absorption spectra of (a) $EuCl_3$-doped and (b) $NiCl_2$-doped PANI film. Key: upper curves, as-prepared films; lower curves, the same films 4 months later.

Electronic absorption spectra of films, especially those doped by the first group of salts, were found to evolve with time. This evolution occurred toward features typical of films with higher conductivity. For example, in samples doped by $EuCl_3$ and $NiCl_2$, we observed a complete disappearance of the BQET band, an increase of the polaron absorption features, and an increase of conductivity up to 1 order of magnitude for a period of 4 months (Figure 3). In this case, the final spectrum was still different from the spectrum of PANI films acid protonated or doped by the second group of salts. The latter films possess a free-carrier absorption tail that begins from ∼500 nm and gradually increases to the IR region, with concomitant suppression of the BQET band. On gradual increase of the protonation level, isosbestic points in electronic spectra are normally present[29] that indicate the coexistence of only two forms of PANI, undoped EB and protonated doped ES. In the above case, two bends are clearly seen in spectra (Figure 3), the first one at ∼500 nm, and the second one at ∼680 nm, from which the free-carrier tail begins to grow rapidly. The free-carrier tail seems to be independent

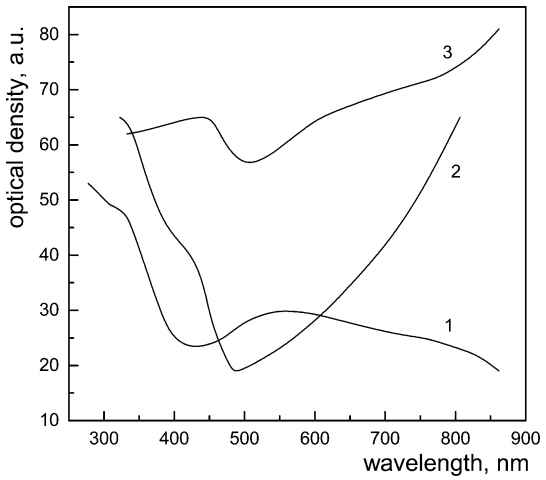

Figure 4. Electronic absorption spectra of (1) $CuCl_2$-doped, (2) $ZnCl_2$-doped, and (3) $Al_2(SO_4)_3$-doped PANI film.

of the presence of the BQET band, so more than two forms of the polymer should be expected in the film during doping.

The other interesting property of the samples was the dependence of their electronic spectra on the film thickness. We compared films of different thickness doped by $EuCl_2$ and $ZnCl_2$, respectively, and found that doping characteristics are dependent on the film thickness. The electronic spectra of thin films showed the absence of polaron absorption features and the presence of PB features, i.e., a blue-shifted band of BQET (Figure 5). On the other hand, spectra of thicker films showed a better efficiency of these films for doping by transition-metal salts. This conclusion is in a good agreement with our previous results showing a higher protonation level of thick films as compared to the thin ones after their exposure to acid solutions under the same conditions.[30] On the other hand, a higher tendency of thin films to oxidation is consistent with our previous observations of oxidation activity of $EuCl_3$ solutions in respect to EB.[6] This phenomenon can be explained by the fact that thinner films were prepared from more diluted solutions, where oxidation of the polymer chains proceeds easier.[6]

3.5. IR Spectra. IR absorption spectra of as-prepared cast films of both pure EB and EB doped by inorganic salts showed typical features of the polymer and NMP. A EB film cast from NMP solution has five major absorption bands of the polymer located at ~1592, 1504, 1288, 1160, and 824 cm^{-1} and also an intense band of the C═O stretching vibrations of NMP at 1680 cm^{-1} (Figure 6). Cast polymer film had a reduced intensity of the 1592 cm^{-1} band as compared with the band at 1504 cm^{-1}, in contrast to the spectrum of the EB powder, where intensities of these two bands are approximately equal. Suppression of the band intensity at 1592 cm^{-1} in the cast film was probably caused by solvation effects. A similar effect was observed in ref 31 and was assigned to the cross-linking of the EB chains.

In films doped by transition-metal salts, the presence of NMP can also be identified through an absorption band of the C═O stretching vibrations. However, the position of this band is red-shifted to the region 1664−1648 cm^{-1} as compared to that in undoped EB films (Figure 6). Such a shift is indicative of solvation of metal cations that coordinate to the solvent via oxygen atom

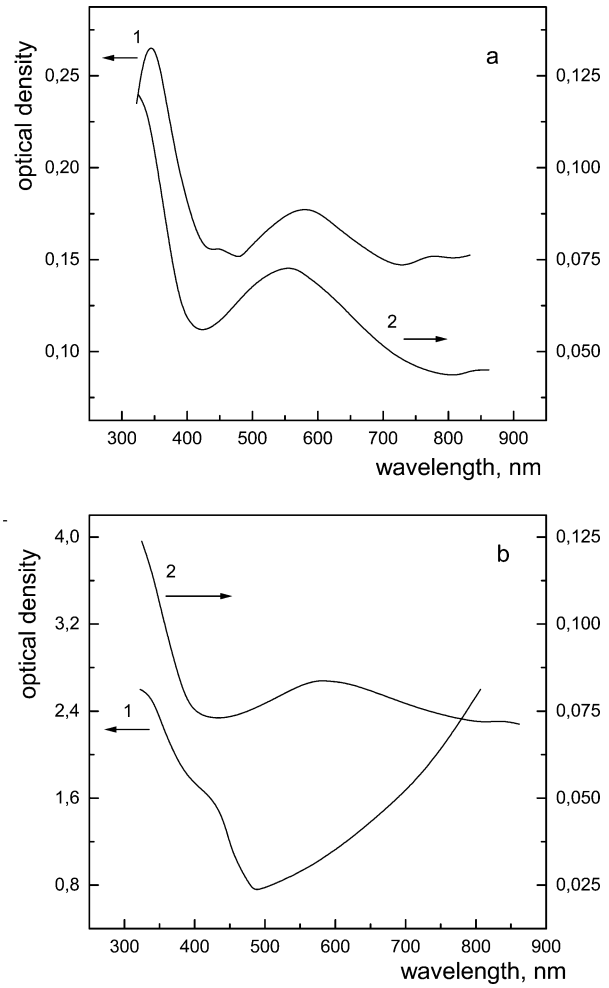

Figure 5. Electronic absorption spectra of (a) $EuCl_3$-doped and (b) $ZnCl_2$-doped PANI film. Key: (1) thick film; (2) thin film.

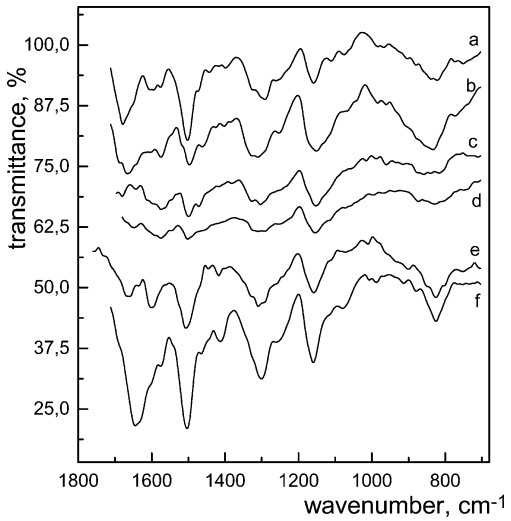

Figure 6. IR absorption spectra of complex polymer films cast from NMP solutions: undoped EB film; (b) $CuCl_2$-doped, (c) $LaCl_3$-doped, (d) $NiCl_2$-doped, (e) $CdCl_2$-doped, and (f) $ZnCl_2$-doped EB films.

of the C═O group.[32] Intensity of the above band varies from sample to sample and shows a gradual decrease with time, reflecting a slow dynamics of solvent release from the film.

It was found that IR spectra also reflect different tendencies of doping mentioned above. Intensity of the

Table 3. Position (in cm^{-1}) of the Main IR Absorption Bands of Films in Figure 6 and Their Assignment According to the Literature Data[33−36]

EB	EB:$CuCl_2$	EB:$LaCl_3$	EB:$NiCl_2$	EB:$CdCl_2$	EB:$ZnCl_2$	assignment
1680	1664			1656		C═O stretching vibration of NMP
1592				1608	1608	C−C stretching of benzenoid ring
	1576	1576	1576			C═C stretching of quinoid ring
1504	1496	1496	1504	1512	1496	ring stretching (CC and CH) + C═N stretching
1288	1312	1304	1312	1312	1312	C−N and $C-N^+$ stretching + C−H bending
1160	1152	1152	1152	1160	1160	C−H bending
824	832	856	832	824	832	C−H out-of-plane bending

NMP band in samples doped by $ZnCl_2$, $CdCl_2$, $FeSO_4$, and lanthanide nitrates was strong, while that in samples doped by $EuCl_3$, $LaCl_3$, and $NiCl_2$ was relatively small. The high-frequency peak of the polymer at ∼1592 cm^{-1} in films doped by $ZnCl_2$ was blue-shifted, so that it merged with the NMP band, while the same peak in samples doped by $EuCl_3$, $LaCl_3$, and $NiCl_2$ was red-shifted to 1576 cm^{-1} (Table 3). The other peculiarity was that equal amounts of the material cast into films yielded different intensity of their IR spectra. The IR absorption bands of samples doped by $EuCl_3$, $LaCl_3$, $NiCl_2$ showed significantly smaller intensities as compared, for example, with the film doped by $ZnCl_2$ (Figure 6). Such a difference points out different structural organization of the polymer chains in the film, i.e., a more dense, compact-coil arrangement in the films doped by the first group of salts, and a more loose, expanded-coil arrangement in the $ZnCl_2$-doped films, which results in different efficiency of the IR absorption.

According to the literature data (see, for example, refs 33 and 34), the oxidized form of the polymer, i.e., PB, should display red-shifted absorption bands at ∼1592, 1504, and 1160 cm^{-1} and a blue-shifted band at ∼1300 cm^{-1}. It should be noted that the $CuCl_2$-doped film just demonstrates the above shifts (Table 3), and the oxidation of the polymer in this film is quite consistent with its electronic spectra (Figure 4). For analysis of the oxidation state of the other samples we consider the absorption band at ∼1592 cm^{-1} in more detail. According to the vibrational analysis of PANI,[33−36] the position of this band can be taken as that indicative of the oxidation degree of the polymer. The origin of this band is due to superposition of the C−C stretching vibration of the benzene ring in the 1596−1600 cm^{-1} range, and of C═C stretching vibration of the quinoid ring in the 1570−1578 cm^{-1} range. Thus, a red-shifted band indicates the increase of the relative number of quinoid groups in the polymer chain. On the basis of this analysis, a partial oxidation of the polymer doped by $EuCl_3$, $LaCl_3$, and $NiCl_2$ should be concluded. This conclusion is also consistent with electronic spectra of these films.

3.6. Salts of Other Metals. In addition to various transition-metal salts used in this work, it was found that salts of other metals can also successfully dope the EB, resulting in a significant increase of conductivity and change in electronic spectra of the doped films. Examples of such salts are $Al_2(SO_4)_3$ and $Pb(NO_3)_2$. These salts cannot be unambiguously related to the dopants of either the first or second group. For example, films doped by $Al_2(SO_4)_3$ have a granular morphology, but electronic spectrum similar to that of films doped by $ZnCl_2$ (Figure 4).

The above results allow to conclude that the *d*-electronic level of transition-metal ions does not play a crucial role in doping of EB chains and changing their physical properties.

4. Discussion

Changes in spectra of electronic absorption and IR absorption, as well as conductivity changes, unambiguously prove doping of the polymer by inorganic salts. The doping induces changes both on the molecular level and on the macroscopic structural level of the films. Both changes affect conductivity of the material.

First, we discuss changes on the molecular level. We distinguish two types of activity of the metal cations in respect to the polymer chains. These two types of activity are related to the two basic groups in the polymer chain, the electron-rich benzenoid group and electron-deficient quinoid group, respectively (Figure 1). Transition-metal ions with relatively low electrode potential, such as Zn^{2+}, coordinate predominantly to nitrogen atoms of the quinoid group, similarly to activity of alkali-metal ions.[3−5] This conclusion is consistent with the obtained electronic and IR absorption spectra of the films. We would like to note that the presence of solvent molecules in the film causes coordination of the cation to both the polymer and solvent molecules (Figure 7a), thus providing a loose arrangement of the polymer chains, similar to the arrangement of polymer coils in solutions.

The other type of activity of metal cations is their ability to coordinate to nitrogen atoms of the benzenoid group. This ability is dependent on the metal electrode potential. Transition-metal ions with relatively high electrode potential, such as Cu^{2+}, are able to directly oxidize benzenoid groups of the polymer, i.e., to induce the EB-to-PB conversion. This conclusion is consistent with the features of the PB observed in the $CuCl_2$-doped PANI films through electronic and IR absorption spectra above, and in $CuCl_2$-doped PANI solutions reported in ref 37. However, it should be noted that the $CuCl_2$-doped film possesses a small IR absorption tail (Figure 4) and conductivity of about 10^{-4} S/cm. These features point out the presence of polarons in the polymer backbone; therefore, the doping of PANI by copper cations should be presented as withdrawal of electrons from the electron-rich benzenoid group with formation of polarons in the polymer backbone.

Finally, we distinguish an intermediate case of the above forms of activity, when metal cations are able to coordinate to both quinoid and benzenoid groups of the polymer. Among transition-metal ions used in this work, we refer this form of activity to nickel and lanthanide cations. Salt anions seem to influence this form of activity also. As was mentioned, films doped by $NiCl_2$, $LaCl_3$, and $EuCl_3$ show the features of both the oxidized polymer chains and highly conductive polymer chains observed in the electronic and IR absorption spectra, along with the relatively high electrical conductivity. These data suggest that the PB and metal-doped forms of PANI coexist in the complex film. To explain this phenomenon, it should be mentioned that the polymer

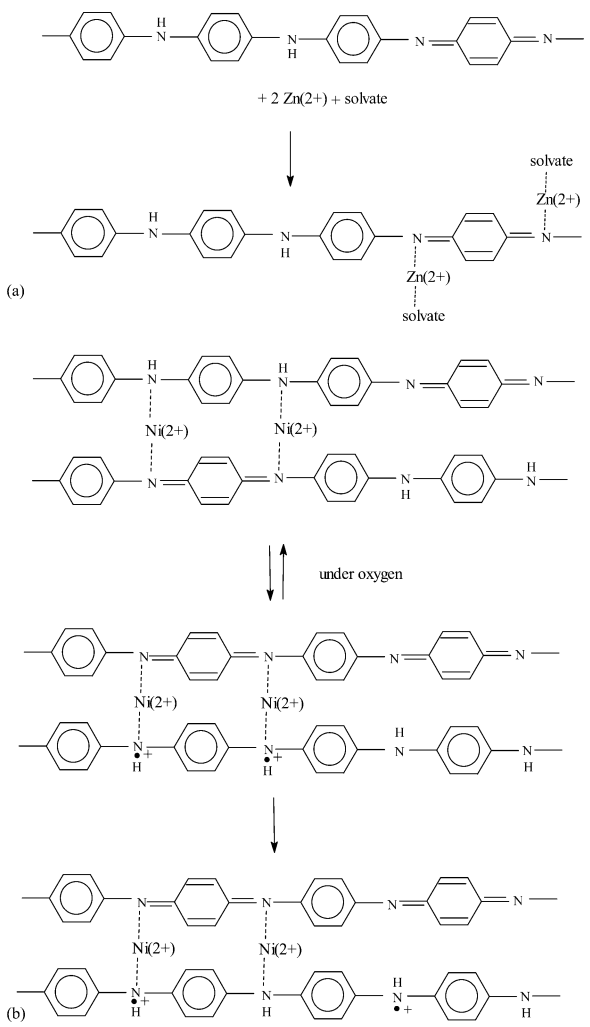

Figure 7. Proposed scheme of the formation of the EB−metal salt complexes (salt anions are not shown): (a) coordination to both polymer and solvent leading to a single-strand system (polaron formation is not shown); (b) conjugated network system.

doped by the above salts has a tendency to precipitate in the solutions,[20] and that such a doping leads to films with a grained morphology. These properties suggest some dense packing of the polymer chains in a film, which can be induced by the interchain coordination of the metal cations. Thus, the interaction of the above cations and the polymer can be schematically presented as coordination of metal cations to nitrogen atoms of both benzenoid and quinoid group of the adjacent chains, reversible *interchain* redox reaction resulting in formation of the adjacent PB and bipolaron ES chains, followed by irreversible polaron separation and formation of the PB and polaron ES chains, respectively (Figure 7b). The second step, i.e., the redox reaction leading to the oxidized polymer chain, is consistent with earlier reported observations that polyaniline serves as a synthetic metal catalyst with a reversible redox function, able to oxidize some species under oxygen atmosphere, for example benzylamines into corresponding imines, and that complexation of PANI with some transition-metal chlorides promotes the above reactions.[17,18] In a similar way, we propose that complex formation of PANI and $NiCl_2$, $LaCl_3$, or $EuCl_3$, stimulates a similar activity, i.e., oxidation of a neighboring PANI chain (Figure 7b). The PB form is unstable in respect to hydrolysis,[25] so its gradual degradation in air seems to be responsible for changes in the electronic spectra and improvement of the film conductivity with time (Figure 3).

Change on the macroscopic level induced by doping leads to formation of films with different morphology. The presence of inorganic salt in the polymer films is essential in formation of their morphological pattern. It is known that inorganic salts form crystals in the solid state. The driving force for crystal formation, i.e., the Coulomb interaction between the ions, seems to be retained, although to a lesser extent, in the doped polymer film. That may be responsible for formation of polymer-inorganic salt grains in the complex film. AFM images of samples doped by the first group of dopants clearly showed the presence of grains forming a fractal continuum in the film (Figure 2a). It appears that polymer chains inside the grain form a conjugated network system (Figure 7b) assisting charge hopping there, therefore these grains are responsible for the relatively high conductivity of the grained films as compared with films doped by salts of the second group, where no grain in the film structure has been found.

5. Conclusions

This study as well as other works[1−12] undoubtedly indicates that doping of EB by metal ions, leading to an increase of conductivity, is a common property. However, there is a difference with respect to which metal cation is used for doping. One can characterize metal cations with regard to their electrode potentials. Transition-metal ions with low electrode potentials, as well as alkali-metal ions,[3−5] attack quinoid units of the polymer, thus resulting in pseudo-protonation of the polymer backbone. Transition-metal ions with high electrode potential, such as Cu^{2+},[37] as well as Pd^{2+} [11] and Au^{3+},[38] to mention just a few, attack predominantly benzenoid groups of the polymer, resulting in the polymer oxidation to the PB. A large group of the transition-metal ions with an intermediate electrode potential seem to be able to interact both with benzenoid and quinoid groups of the polymer backbone, inducing a relatively high conductivity of the material.

An important consequence of doping of the EB films by transition-metal salts is the change of their morphology. The role of the counterion in these changes is also important. Chlorides of some transition metals result in a grained morphology of the complex films with their relatively high conductivity, while nitrates of the same metals lead to a far smaller conductivity and a higher solvent residue in the films. Thus, transition-metal salts can be used as dopants of PANI, inducing both molecular and morphological changes of the film.

Acknowledgment. The author is grateful to Mrs. O. Lytvyn for measurements and treatment of AFM images of the films.

References and Notes

(1) Kulszewicz-Bajer, I.; Pron, A.; Abramowicz, J.; Jeandey, C.; Oddou, J.-L.; Sobczak, J. W. *Chem. Mater.* **1999**, *11*, 552.
(2) Chaudhuri, D.; Kumar, A.; Rudra, I..; Sarma, D. D. *Adv. Mater.* **2001**, *13*, 1548.
(3) Saprigin, A. V.; Brenneman, K. R.; Lee, W. P.; Long, S. M.; Kohlman, R. S.; Epstein, A. J. *Synth. Met.* **1999**, *100*, 55.
(4) Chen, S. A.; Liang, L.-C. *Macromolecules* **1995**, *28*, 1239.
(5) Chen, S.-A.; Lin, L.-C. *Adv. Mater.* **1995**, *7*, 473.
(6) Dimitriev, O. P.; Kislyuk, V. V. *Synth. Met.* **2002**, *132*, 87.

(7) MacDiarmid, A. G.; Epstein, A. J. *Faraday Discuss. Chem. Soc.* **1989**, *88*, 317.
(8) Cai, L.-T.; Yao, S.-B.; Zhou, S.-M. *Synth. Met.* **1997**, *88*, 205.
(9) Anand, J.; Rao, P. S.; Palaniappan, S.; Sathyanarayana, D. N. *Synth. Met.* **1998**, *95*, 57.
(10) Genoud, F.; Kulszewicz-Bajer, I.; Bedel, A.; Oddou, J.-L.; Jeandey, C.; Pron, A. *Chem. Mater.* **2000**, *12*, 744.
(11) Hasik, M.; Drelinkiewicz, A.; Wenda, E. *Synth. Met.* **2001**, *119*, 325.
(12) Dominis, A. J.; Spinks, G. M.; Kane-Maguire, L. A. P.; Wallace, G. G. *Synth. Met.* **2002**, *129*, 165.
(13) Paloheimo, J.; Laakso, K.; Isotalo, H.; Stubb, H. *Synth. Met.* **1995**, *68*, 257.
(14) Epstein, A. J.; Smallfield, A. O.; Guan, H.; Fahlman, M. *Synth. Met.* **1999**, *102*, 1374.
(15) Fahlman, M.; Crispin, X.; Guan, H.; Li, S.; Smallfield, A. O.; Wei, Y.; Epstein, A. J. *Polym. Prepr.* **2000**, *41*, 1753.
(16) Posdorfer, J.; Wessling, B. *Synth. Met.* **2001**, *119*, 363.
(17) Higuchi, M.; Ikeda, I.; Hirao, T. *J. Org. Chem.* **1997**, *62*, 1072.
(18) Hirao, T. *Coord. Chem. Rev.* **2002**, *226*, 81.
(19) Price, W. E.; Ralph, S. F.; Wallace, G. G. *Aust. J. Chem.* **2001**, *54*, 615.
(20) Dimitriev, O. P. *Polym. Bull. (Berlin)* **2003**, *50*, 83.
(21) Montrel, M. M.; Stroustrup, N. *Macromol. Rapid Commun.* **2002**, *23*, 1134.
(22) Smertenko, P. S.; Dimitriev, O. P.; Schrader, S.; Brehmer, L. Submitted for publication.
(23) Rannoua, P.; Nechtschein, M.; Travers, J. P.; Berner, D.; Wolter, A.; Djurado, D. *Synth. Met.* **1999**, *101*, 734.
(24) Masters, J. G.; Sun, Y.; MacDiarmid, A. G. *Synth. Met.* **1991**, *41*, 715.
(25) Leng, J. M.; McCall, R. P.; Cromack, K. R.; Sun, Y.; Manohar, S. K.; MacDiarmid, A. G.; Epstein, A. J. *Phys. Rev. B* **1993**, *41*, 15719.
(26) Stafstrom, S.; Bredas, J. L.; Epstein, A. J.; Woo, H. S.; Tanner, D. B.; Huang, W. S.; MacDiarmid, A. G. *Phys. Rev. Lett.* **1987**, *59*, 1464.
(27) MacDiarmid, A. G.; Chiang, J. C.; Richter, A. F.; Epstein, A. J. *Synth. Met.* **1987**, *18*, 286.
(28) Wudl, F.; Angus, R. O.; Lu, F. L.; Allemand, D. M.; Vachon, D. J.; Nowak, M.; Liu, Z. X.; Heeger, A. J. *J. Am. Chem. Soc.* **1987**, *109*, 3677.
(29) Dimitriev, O. P.; Getsko, O. M. *Synth. Met.* **1999**, *104*, 27.
(30) Dimitriev, O. P. *Synth. Met.* **2001**, *122*, 315.
(31) Lu, X.; Tan, C. Y.; Xu, J.; He, C. *Synth. Met.* **2003**, *138*, 429.
(32) Krishnamurthy, S. S.; Saundararajan, S. *J. Inorg. Nucl. Chem.* **1966**, *28*, 1689.
(33) Quillard, S.; Louarn, G.; Lefrant, S.; MacDiarmid, A. G. *Phys. Rev. B* **1994**, *59*, 12496.
(34) Cochet, M.; Corraze, B.; Quillard, S.; Buisson, J. P.; Lefrant, S.; Louarn, G. *Synth. Met.* **1997**, *84*, 757.
(35) Quillard, S.; Louarn, G.; Buisson, J. P.; Boyer, M.; Lapkowski, M.; Pron, A.; Lefrant, S. *Synth. Met.* **1997**, *84*, 805.
(36) Pereira da Silva, J. E.; Cordoba de Torresi, S. I.; de Faria, D. L. A.; Temperini, M. L. A. *Synth. Met.* **1999**, *101*, 834.
(37) Higuchu, M.; Imoda, D.; Hirao, T. *Macromolecules* **1996**, *29*, 8277.
(38) Neoh, K. G.; Young, T. T.; Looi, N. T.; Kang, E. T.; Tan, K. L. *Chem. Mater.* **1997**, *9*, 2906.

MA035677W